Journal of Zhejiang University SCIENCE A
ISSN 1673-565X (Print); ISSN 1862-1775 (Online)
www.zju.edu.cn/jzus; www.springerlink.com
E-mail: jzus@zju.edu.cn

Research on the operating characteristics of parallel 4-DOF electric platform with 4TPS-PS structure*

CHENG Jia†, WANG Xuan-yin†‡, FU Xiao-jie, LI Qiang

(*The State Key Laboratory of Fluid Power Transmission and Control, Zhejiang University, Hangzhou 310027, China*)

†E-mail: chengjiazju@gmail.com; xywang@zju.edu.cn

Received Nov. 29, 2006; revision accepted Mar. 9, 2007

Abstract: The 4TPS-PS parallel platform designed for a stabilization and automatic tracking system is a novel lower-mobility parallel mechanism. In the first part of this paper, the structure of the platform is described and the kinematics model is built. The workspace of the platform is defined as the full reachable rotation workspace when the *Z* coordinate dimension of the upper plate varies continuously. A fast searching method of the full reachable workspace is presented, after which the inverse kinematics of the platform is deduced. The forward and inverse solutions of the speed and force of the platform are deduced. According to the characteristic of the 4TPS-PS platform's structure, a fast searching algorithm of the maximum generalized speed and maximum generalized force output by the upper plate is put forward based on the forward and inverse solutions of the platform's speed and force. The 4TPS-PS platform prototype built by the State Key Laboratory of Fluid Power Transmission and Control of China is taken as the research subject. The full reachable rotation workspace of the prototype is computed out and analyzed. The curves of maximum generalized speed and maximum generalized force of the prototype are computed out and plotted. Finally, the computing and analyzing results of the operating characteristics are confirmed through the experiment.

Key words: Parallel mechanism, 4-DOF, Workspace, Generalized speed, Generalized force
doi:10.1631/jzus.2007.A1800 **Document code:** A **CLC number:** TH13

INTRODUCTION

In 1947, Dr. Eric Gough, a British engineer designed a kind of 6-DOF (degree of freedom) parallel mechanism to test tires (Bonev, 2003). In 1965, Mr. Stewart in Germany designed a flight simulator using similar structure, and issued a famous paper that was widely referred to (Bonev, 2003). In 1978, Professor Hunt in Australia popularized the parallel mechanism to the robot field (Dasgupta and Mruthyunjaya, 2000), and then the parallel mechanism began to be studied and used extensively. Compared to the series mechanism, the parallel mechanism has many advantages including high rigidity, powerful load capacity, good structure stiffness, high control precision, quick response, low mass power rate, etc., but its workspace is much smaller. The parallel mechanism is widely used in motion simulator, robot, parallel kinematics machine tool, docking simulating test device, sensors, etc. (Bonev, 2003; Dasgupta and Mruthyunjaya, 2000).

So far, the 6-DOF parallel mechanism has matured to a point. Lower-mobility parallel mechanism including 2-, 3-, 4- and 5-DOF parallel mechanism has some advantages compared to the 6-DOF parallel mechanism, such as simple structure, low costs, and easy control. So, in recent years the lower-mobility parallel mechanism has become the research focus of this field, and many kinds of novel structures have been designed, such as 3-RPS, 3-UPU, 3-RRR sphere mechanism, Delta mechanism, Tricept mechanism, etc. (Gao *et al*., 2002; Huang and Li, 2003; Joshi and Tsai, 2003; Liu *et al*., 2005; Shen *et al*., 2005; Zhang and Gosselin, 2002; Li *et al*., 2005; Huang *et al*., 1997).

‡ Corresponding author
* Project (No. 50375139) supported by the National Natural Science Foundation of China

The pointing directions of the equipments on vehicles are disturbed by the movements including roll, pitch, heading, vibration when vehicles are moving on. The stabilization and automatic tracking system which is widely used can insulate the motion of vehicles (Cheng *et al*., 2006). A novel 4TPS-PS parallel platform shown in Fig.1 has been designed by the State Key Laboratory of Fluid Power Transmission and Control of China for the stabilization and automatic tracking system, which is a novel lower-mobility parallel mechanism with 4-DOF including rotations around three coordinate axes and translation along one coordinate axis. The operating characteristics of the platform including workspace, generalized speed and generalized force are studied in this paper.

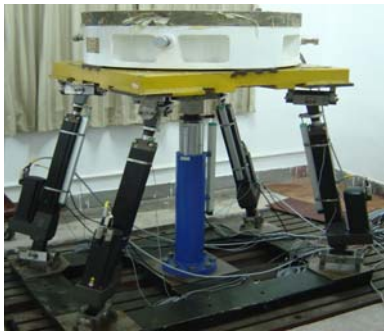

Fig.1 Photo of the 4-DOF parallel platform prototype with 4TPS-PS structure

MECHANISM DESCRIPTION AND KINEMATICS MODELLING

The structure of the 4TPS-PS platform is shown in Fig.2. The platform consists of the upper plate, the base plate, four same actuating legs and one slave leg. The upper plate is connected with the base plate by four electric cylinders and one slave leg. One end of an electric cylinder is connected with the base plate by a Hooke joint, and the other end is connected with the upper plate by a spherical joint. Four Hooke joints A_1, A_2, A_3, A_4 made up of an inscribed rectangle of the circle whose radius is R_0, and four spherical joints B_1, B_2, B_3, B_4 made up of an inscribed rectangle of the circle whose radius is R_1. The electric cylinders are actuated by servomotors. The slave leg is composed of two components. The upper component is connected with the upper plate by a spherical joint. The end of the lower component is fixed with the base plate. And the two components are connected by a prismatic pair. The structure of the 4TPS-PS parallel platform is determined by five parameters including R_0, R_1, the distributing angles of the joints in the base and upper plates θ_0, θ_1 ($\theta_0 \neq \theta_1$) and the initial height of the platform H_0.

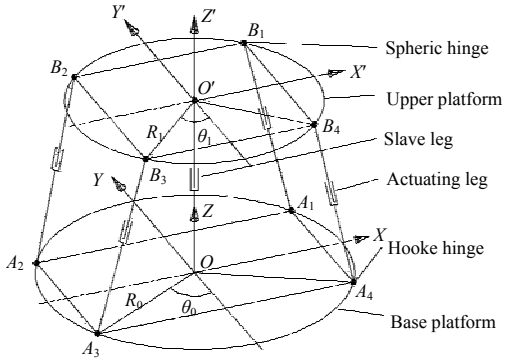

Fig.2 Schematic map of the 4TPS-PS parallel platform

According to Kutzbach Crubler's formula (Huang *et al*., 1997), the platform has 4-DOF. The upper plate can rotate around three coordinate axes and translate along one coordinate axis by the lengthening or shortening of four electric cylinders, and the four motions can be realized individually or coupled. The slave leg restricts two translations along X', Y' axes of the upper plate, the upper component of which can translate along Z axis passively.

As illustrated in Fig.2, the moving reference frame and the base reference frame are established. The moving frame (O'-$X'Y'Z'$) is fixed to the upper plate, where point O' is located at the center of the rectangle $B_1B_2B_3B_4$. The base reference frame (O-XYZ) is fixed to the base plate, where point O is located at the center of the rectangle $A_1A_2A_3A_4$. The distance between point O and A_1, A_2, A_3, A_4 equals R_0. The distance between point O' and B_1, B_2, B_3, B_4 equals R_1.

The coordinates of the points A_1, A_2, A_3, A_4 in the base reference frame are:

$$\boldsymbol{A}=[\boldsymbol{A}_1, \boldsymbol{A}_2, \boldsymbol{A}_3, \boldsymbol{A}_4], \tag{1}$$

where $\boldsymbol{A}_i=[k_{xi}R_0\sin\theta_0,\ k_{yi}R_0\cos\theta_0,\ 0]^{\mathrm{T}}$ (i=1,2,3,4; $k_{x1}=k_{x4}=k_{y1}=k_{y2}=1$; $k_{x2}=k_{x3}=k_{y3}=k_{y4}=-1$).

The coordinates of the points B_1, B_2, B_3, B_4 in the

moving reference frame are:

$$\boldsymbol{B}'=[\boldsymbol{B}_1', \boldsymbol{B}_2', \boldsymbol{B}_3', \boldsymbol{B}_4'], \tag{2}$$

where $\boldsymbol{B}_i'=[k_{xi}R_1\sin\theta_1,\ k_{yi}R_1\cos\theta_1,\ 0]^{\mathrm{T}}$ (i=1,2,3,4; $k_{x1}=k_{x4}=k_{y1}=k_{y2}=1$; $k_{x2}=k_{x3}=k_{y3}=k_{y4}=-1$).

SOLUTION OF THE FULL REACHABLE ROTATION WORKSPACE

When the 4TPS-PS platform is used in the stabilization and automatic tracking system, its primary operating modes are rotations around three coordinate axes. So the ranges of the three rotations when the Z coordinate dimension of the upper plate (viz. Z_c) varies unlimitedly are defined as the full reachable rotation workspace of the platform, and the angles of rotations around X', Y', Z' axes (γ, β, α) are defined as the x, y, z axes of the rotation workspace. The rotation workspace of the platform can be rapidly searched out by using the inverse kinematics.

The process of the inverse kinematics is as follows:

The coordinates of the points B_1, B_2, B_3, B_4 in the moving reference frame are transformed to the coordinates in the base reference frame:

$$\boldsymbol{B}=\boldsymbol{Q}\cdot\boldsymbol{B}'+\boldsymbol{P}, \tag{3}$$

where $\boldsymbol{B}$ stands for the coordinates of the points B_1, B_2, B_3, B_4 in the base reference frame, $\boldsymbol{Q}$ stands for the orientation cosine matrix of the moving reference frame with respect to the base frame, $\boldsymbol{P}$ stands for the coordinates of O' in the base coordinate frame.

$$\boldsymbol{B}=[\boldsymbol{B}_1, \boldsymbol{B}_2, \boldsymbol{B}_3, \boldsymbol{B}_4], \tag{4}$$

$$\boldsymbol{P}=[0\ \ 0\ \ Z_c]^{\mathrm{T}}, \tag{5}$$

$$\boldsymbol{Q}=\begin{bmatrix} i_x & i_y & i_z \\ j_x & j_y & j_z \\ k_x & k_y & k_z \end{bmatrix}, \tag{6}$$

where $i_x=\cos\alpha\cos\beta$, $i_y=\cos\alpha\sin\beta\sin\gamma-\sin\alpha\cos\gamma$, $i_z=\cos\alpha\sin\beta\cos\gamma+\sin\alpha\sin\gamma$, $j_x=\sin\alpha\cos\beta$, $j_y=\sin\alpha\sin\beta\sin\gamma+\cos\alpha\cos\gamma$, $j_z=\sin\alpha\sin\beta\cos\gamma-\cos\alpha\sin\gamma$, $k_x=-\sin\beta$, $k_y=\cos\beta\sin\gamma$, $k_z=\cos\beta\cos\gamma$.

Displacements of four electric cylinders can be computed out easily by the following expression:

$$L_i=|\boldsymbol{B}_i-\boldsymbol{A}_i|,\ i=1, 2, 3, 4. \tag{7}$$

The criterions of the workspace boundary include the displacement limits of the actuating legs, the rotation limits of the joints and the interferences between legs (Gosselin, 1990; Wang *et al*., 2001; Tsai and Lin, 2006). In this paper, the displacement limits are used for searching the workspace; the rotation limits and interferences are used for checking after searching.

The searching process of the platform's rotation workspace is as follows:

(1) Computing out the range of the translating of the upper plate, viz. the range of Z_c.

(2) The range of z viz. angle α is computed out when Z_c varies unlimitedly, and z is used as the first dimension of searching variables. The searching space is divided into a certain number of subspaces with the same thickness Δz along z axis. As illustrated in Fig.3, polar reference frames are established in all section planes, which are parallel to x-y plane, the distance between a point q in the polar reference frames and the zero point O of the polar reference frames is defined as the polar radius, and the polar radius $\rho=\sqrt{\gamma^2+\beta^2}$, and the angle between ρ and x axis is defined as polar angle θ.

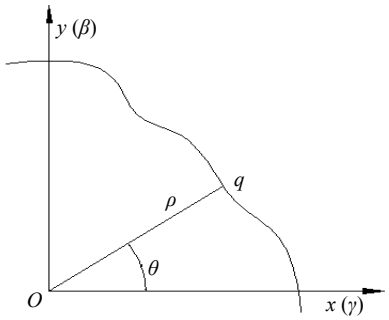

Fig.3 The polar reference frame

(3) The fast searching algorithm in polar coordinate plane is used when the boundary of the sub-workspace is in the process of being ascertained. θ is used as the second searching variable, whose range is [0, 2π]. The boundary of the sub-workspace when $\theta\in[0,\pi/2]$ is first searched out because of the symmetry of the structure, while Z_c varies unlimitedly. The maximum of ρ is $\rho_{\max}(i, j)$ (i denotes the change of α, j denotes the change of θ). The process of

searching in the polar plane is as follows: First, search out the maximum of polar radius in the direction of θ=0, viz. $\rho_{max}(i, 0)$, then increase the polar angle and search out the value of $\rho_{max}(i, j)$ (j>0), whose initial value is set to be $\rho_{max}(i, j-1)$. Until the lengths of the electric cylinders are equal to the limits, do as follows: if the lengths of the electric cylinders are less than the limits, increase the value of $\rho_{max}(i, j)$; otherwise decrease the value. After getting $\rho_{max}(i, j)$, increase the value of θ and do the same as before until $\theta=\pi/2$.

(4) Get the polar radius when $\theta\in[\pi/2,2\pi]$ by mirror copying the polar radius when $\theta\in[0,\pi/2]$.

SOLUTION OF THE SPEED AND OUTPUT FORCE

What we need to know is the maximum generalized speed and maximum generalized force of the upper plate when upper plate is in any pose. According to the characteristic of the 4TPS-PS platform's structure, a method based on the forward and inverse solutions of the platform' speed and force is put forward to quickly solve the generalized speed and generalized force of the upper plate when the largest speed and output force of the electric cylinder are given.

The translation speed of the reference point O' is $\boldsymbol{v}=[0, 0, v_z]^{\mathrm{T}}$. The rotation speed of the upper plate is $\boldsymbol{\omega}=[\omega_x, \omega_y, \omega_z]^{\mathrm{T}}$. The vectors of four electric cylinders are $\boldsymbol{l}_i$ (i=1~4), the unit vectors are $\boldsymbol{e}_i=\boldsymbol{l}_i/L_i$, and the speeds are $\dot{\boldsymbol{l}}_i$. The three-dimensional vectors in the base reference frame of $\boldsymbol{O'B}$ are $\boldsymbol{r}_i$, the speed of joint B_i is $\boldsymbol{v}_{bi}$, and $\dot{\boldsymbol{l}}_i$ are projections in the direction of $\boldsymbol{e}_i$ of $\boldsymbol{v}_{bi}$:

$$\dot{\boldsymbol{l}}_i=\boldsymbol{e}_i\cdot\boldsymbol{v}_{bi}=\boldsymbol{e}_i\cdot\boldsymbol{v}+\boldsymbol{e}_i\cdot(\boldsymbol{\omega}\times\boldsymbol{r}_i). \tag{8}$$

The simplified representation is:

$$\dot{\boldsymbol{l}}=\boldsymbol{J}^{-1}[v_z \quad \boldsymbol{\omega}^{\mathrm{T}}]^{\mathrm{T}}. \tag{9}$$

So the generalized speed of the upper plate is:

$$\boldsymbol{V}_h=[v_z \quad \boldsymbol{\omega}^{\mathrm{T}}]^{\mathrm{T}}=\boldsymbol{J}\cdot\dot{\boldsymbol{l}}, \tag{10}$$

where $\dot{\boldsymbol{l}}=[\dot{\boldsymbol{l}}_1,\dot{\boldsymbol{l}}_2,\dot{\boldsymbol{l}}_3,\dot{\boldsymbol{l}}_4]^{\mathrm{T}}$, $\boldsymbol{J}$ is the Jacobian matrix of the platform, which is related to the structural parameters and the position and pose of platform, and

$$\boldsymbol{J}=\left(\begin{bmatrix} e_{1z} & e_{2z} & e_{3z} & e_{4z} \\ \boldsymbol{r}_1\times\boldsymbol{e}_1 & \boldsymbol{r}_2\times\boldsymbol{e}_2 & \boldsymbol{r}_3\times\boldsymbol{e}_3 & \boldsymbol{r}_4\times\boldsymbol{e}_4 \end{bmatrix}^{\mathrm{T}}\right)^{-1}. \tag{11}$$

When $\boldsymbol{J}$ is not singular, Eqs.(10) and (11) describe the mapping relation between the generalized speed of the upper plate and the speeds of four electric cylinders. When the cylinders' speeds are known, the upper plate's generalized speed can be deduced by using Eqs.(10) and (11). Dually, the cylinders' speeds can be deduced from the upper plate's generalized speed.

The generalized force output by the upper plate is $\boldsymbol{F}=\{F_z, M_x, M_y, M_z\}^{\mathrm{T}}$ (hereinafter referred to as "output force") (Peng and Gao, 2006). The actuating forces of the four electric cylinders are $\boldsymbol{f}=\{f_1, f_2, f_3, f_4\}^{\mathrm{T}}$, which are defined as the input forces of the parallel platform. The force equation of the input and output forces according to the Screw theory (Huang *et al*., 1997) is as follows:

$$\boldsymbol{F}=[\boldsymbol{G}_f^F]\boldsymbol{f}, \tag{12}$$

$$[\boldsymbol{G}_f^F]=\begin{bmatrix} \left(\frac{B_1-A_1}{|B_1-A_1|}\right)_z & \left(\frac{B_2-A_2}{|B_2-A_2|}\right)_z & \left(\frac{B_3-A_3}{|B_3-A_3|}\right)_z & \left(\frac{B_4-A_4}{|B_4-A_4|}\right)_z \\ \frac{A_1\times B_1}{|B_1-A_1|} & \frac{A_2\times B_2}{|B_2-A_2|} & \frac{A_3\times B_3}{|B_3-A_3|} & \frac{A_4\times B_4}{|B_4-A_4|} \end{bmatrix}. \tag{13}$$

When $\boldsymbol{G}_f^F$ is not singular, the output force $\boldsymbol{F}$ can be deduced from actuating forces by using Eqs.(12) and (13). Dually, actuating forces can be deduced from $\boldsymbol{F}$. There is a duality between motion transfer and the static transfer in the theory of mechanisms. The relation between the Jacobian matrix $\boldsymbol{J}$ and the static Jacobian matrix $\boldsymbol{G}_f^F$ is (Huang *et al*., 1997):

$$\boldsymbol{J}=([\boldsymbol{G}_f^F]^{-1})^{\mathrm{T}}. \tag{14}$$

The process of solving the maximum generalized speed and maximum generalized force of the platform is as follows:

(1) When the upper plate translates along Z axis, setting the speeds of four electric cylinders to be max,

the maximum speed of the upper plate can be computed out by forward speed solution. Setting the output forces of four electric cylinders to be max, the maximum output force of the upper plate can be computed out by forward force solution.

(2) The maximum generalized speeds of the upper plate can be solved as follows: Take rotating around X' for example, first set the speed of No. 1 and No. 2 cylinders to be max in positive direction, and set the speed of No. 3 and No. 4 cylinders to be max in negative direction, then calculate the generalized speed of the upper plate by using forward speed solution, which results from coupled multiple DOF motion in most situations. But what we need is the speed of single DOF of the plate. Next step, doing as follows until the speeds of the electric cylinders are equal to the limit to searching out the maximum speed of rotating around X': if the speeds of the electric cylinders are less than the limits, increase the value of the rotating speed around X', otherwise decrease the value. Because the speed of upper plate in positive direction is equal to the speed in the negative direction, only one maximum speed needs to be computed. The maximum rotating speeds around Y' and Z' axes can be solved by the similar method; the differences are that the speed of No. 2 and No. 3 cylinders is set to be max in positive direction and the speed of No. 1 and No. 4 cylinders is set to be max in negative direction when solving the rotating speed around Y' axis, and that the speed of No. 1 and No. 3 cylinders is set to be max in positive direction and the speed of No. 2 and No. 4 cylinders is set to be max in negative direction when solving the rotating speed around Z' axis.

(3) The maximum generalized forces of the upper plate can be solved by using the same method as (2).

OPERATION CHARACTERISTICS OF THE 4TPS-PS PLATFORM

Computing and analyzing of the full reachable rotation workspace

The 4TPS-PS parallel platform prototype built by the State Key Laboratory of Fluid Power Transmission and Control of China is shown in Fig.1. The structure parameters of the platform prototype are as follows: R_0=0.8 m, R_1=0.56 m, θ_0=60°, θ_1=45°, middle height H_0=1.28 m, the stroke of the electric cylinder is 0.45 m. The full reachable rotation workspace is searched out and plotted out in Fig.4 by using the fast searching algorithm described in the second part of this paper. The rotation ranges of upper plate when the height of the upper plate varies are shown in the curves of Fig.5. Users can adjust the height of the plate according to the working demands and the curves. Fig.5a shows the maximum rotating angle curve of each single-degree-of-freedom motion. From Fig.5a, it can be seen that the maximum rotating angles around X' and Y' axes appear when the height of the upper plate approaches to the median value, and the maximum rotating angle around Z' axis appears

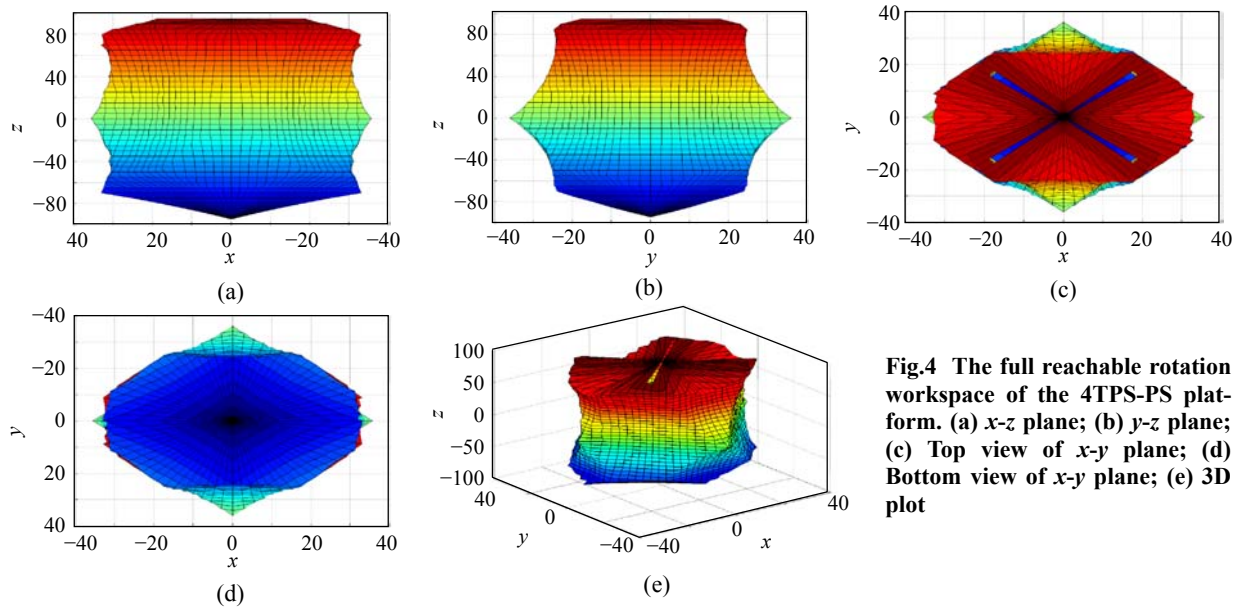

Fig.4 The full reachable rotation workspace of the 4TPS-PS platform. (a) *x*-*z* plane; (b) *y*-*z* plane; (c) Top view of *x*-*y* plane; (d) Bottom view of *x*-*y* plane; (e) 3D plot

when the height of the plate is equal to the minimal value, and the angle around Z' axis decreases with the upper plate lifting. Fig.5b shows the maximum coupled rotating angle curves, and it can be seen that the maximum rotating angles vary little with the height of the upper plate changing.

From above it can be concluded that the rotation workspace of the 4TPS-PS platform has following characteristics: (1) The rotation angle range of the upper plate is wide, especially the angle of the rotation around Z' can exceed 90°, which can not be achieved by Gough-Stewart 6-DOF platform; (2) The rotation workspaces around X' and Y' axes of the platform are almost symmetrical; (3) With the angle of rotating around Z' axis (viz. α) changing, γ and β change little. These three characteristics are exactly what the stabilization and automatic tracking system needs.

Computing and analyzing of the generalized speed of the upper plate

The maximum speed of the electric cylinder is 0.55 m/s. Fig.6 shows the speed curves of 4-DOF of the platform with the position and pose of the upper plate varying. In Fig.6, the unit of the translation speed along Z axis is cm/s and the units of other rotating speeds are °/s. From Fig.6, it is clear that with the position and pose of the upper plate changing the speed of rotating around Z' axis is relatively fast and varies much, but speeds of translation along Z axis and rotation around X' and Y' axes change little.

Computing and analyzing of the generalized force of the upper plate

The maximum output force of the electric cylinder is 20 kN. Fig.7 shows the output force curves of

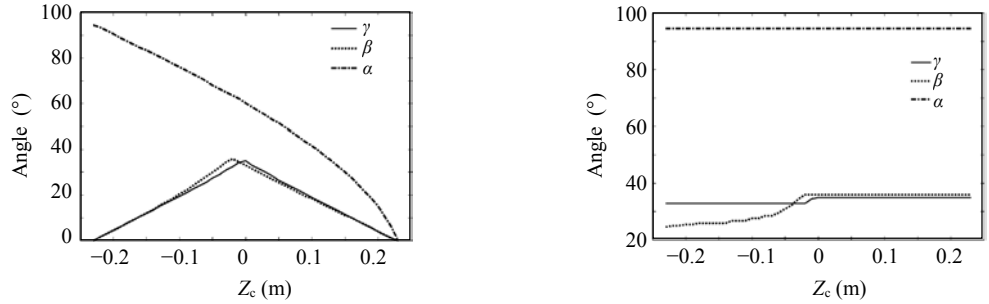

Fig.5 The relation between the workspace and the height of the upper plate (viz. Z_c). (a) Maximum angle of the single-degree-of-freedom rotation; (b) Maximum angle of the coupled rotation

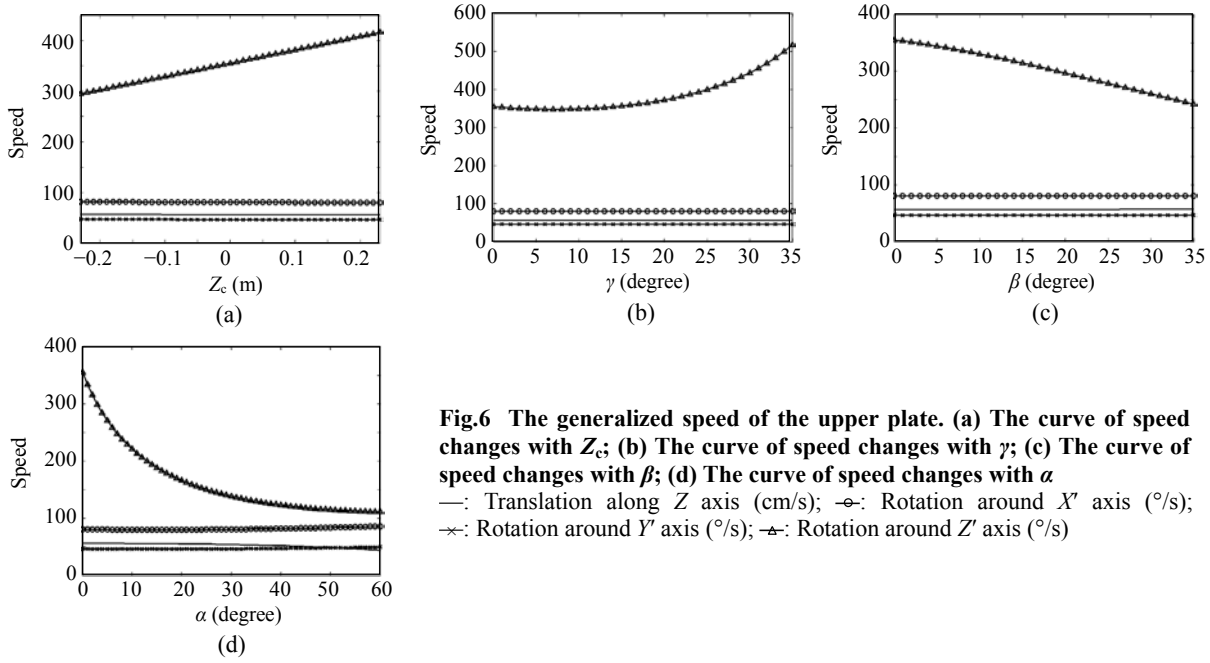

Fig.6 The generalized speed of the upper plate. (a) The curve of speed changes with Z_c; (b) The curve of speed changes with γ; (c) The curve of speed changes with β; (d) The curve of speed changes with α

—: Translation along Z axis (cm/s); -o-: Rotation around X' axis (°/s); -×-: Rotation around Y' axis (°/s); -△-: Rotation around Z' axis (°/s)

the platform with the position and pose of the upper plate varying. In Fig.7, the unit of the force along Z axis is kN and the unit of other torque is kN·m. From Fig.7, it is clear that the generalized force output by the platform is big, but the torque around Z' axis is relatively small, the generalized force of the platform varies little with the position and pose of the upper plate varying, but because the range of rotating around Z' axis is big enough, when α is equal to a big value, the output force reduces relatively more.

EXPERIMENT

There are four movements of the upper plate which need to be measured including the displacement of the translation along Z axis (viz. Z_c), the angles of rotation around X', Y', Z' axes. The height of the upper plate (viz. Z_c) is obtained by the rectilinear displacement transducer fixed on the slave leg, and the displacement transducer's range is 500 mm, its resolution is infinite, and its precision is 0.05%. According to the demands of the stabilization and automatic tracking system, an attitude and heading reference system is installed on the upper plate, which is used to measure the absolute angle value of the upper plate's attitude and heading (viz. γ, β, α), and its performances are shown in Table 1. The control system of the platform consists of an industrial computer and a motion controller UMAC. The industrial computer does the inverse kinematics solution, and gets the feedback of sensors to detect the height, attitude and heading of the upper plate. While the motion controller UMAC real-time controls the motion of the four electric cylinders.

Table 1 The performances of the attitude and heading reference system

	Range (°)	Resolution (°)	Static accuracy (°)
Roll	±180	0.1	0.3
Pitch	±90	0.1	0.3
Heading	±180	0.1	0.5

During the experiment, the platform moves smoothly and steadily, and there is no interference in joint hinges or between electric cylinders when the upper plate moves to the limited position and pose. The maximum rotation workspace of the platform

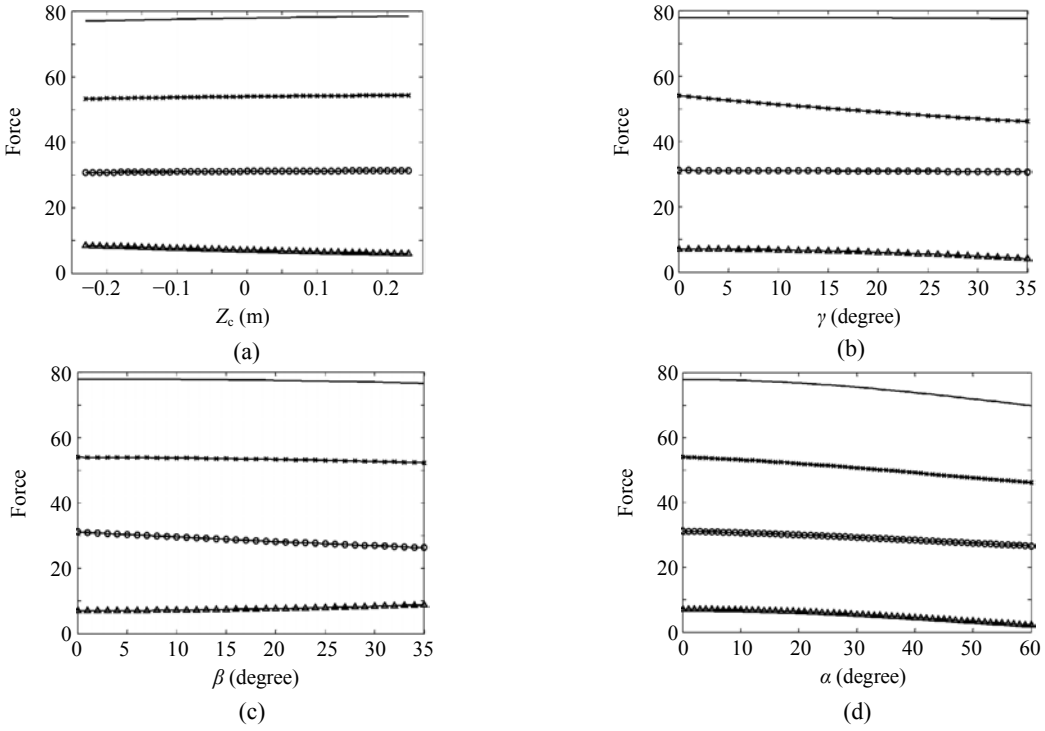

Fig.7 The generalized force of the upper plate. (a) The curve of output force changes with Z_c; (b) The curve of output force changes with γ; (c) The curve of output force changes with β; (d) The curve of output force changes with α
—: Translation along Z axis (kN); -o-: Rotation around X' axis (kN·m); -×-: Rotation around Y' axis (kN·m); -△-: Rotation around Z' axis (kN·m)

measured in experiments matches well with the workspace computed out in Section 4 of this paper, such as the simulation and actual ranges of the rotation around X' axis both are about ±35°, the error is less than 0.5°. Because the computing precision of the workspace is due to the precision of the structure parameters and the stroke of the electric cylinders, the consistence between the actual and theoretical workspaces indicates that the manufacturing and assembling precision of the platform is very high. And the computing accuracies of the speed and force of the platform are due to the Jacobian matrix of the platform, which is determined only by the structure parameters, the current position and pose of the platform. So it can be deduced that the result of computing and analyzing about the speed and force of the platform in Section 4 is correct and can be referred to.

CONCLUSION

The 4TPS-PS parallel platform is a novel lower-mobility parallel mechanism, whose upper plate can rotate around three coordinate axes and translate along Z axis. According to the demands of the stabilization and automatic tracking system and the structural characteristics of the platform, the workspace of the platform was defined as the full reachable rotation workspace in this paper. The fast searching algorithm of the full reachable rotation workspace and the fast solving method of the generalized speed and generalized force are put forward. By computing, analyzing and experiments, it can be concluded that the 4TPS-PS platform has the following operating characteristics: the rotation workspace is large, the generalized speed and output generalized force are large and change little in the workspace, and the operating characteristics of the 4TPS-PS platform can meet the demands of the stabilization and automatic tracking system.

References

Bonev, I., 2003. The True Origins of Parallel Robots. Http://www.parallemic.org/

Cheng, J., Wang, X.Y., Li, Q., Tong, N.J., 2006. Dimensional Synthesis of 4TPS-1PS Parallel Platform Using Genetic Algorithms. Proceedings of the 7th International Conference on Frontiers of Design and Manufacturing. Sydney, Australia, p.443-446.

Dasgupta, B., Mruthyunjaya, T.S., 2000. The Stewart platform manipulator: A review. *Mechanism and Machine Theory*, **35**(1):15-40. [doi:10.1016/S0094-114X(99)00006-3]

Gao, F., Li, W.M., Zhao, X.C., Jin, Z.L., Zhao, H., 2002. New kinematic structures for 2-, 3-, 4-, and 5-DOF parallel manipulator designs. *Mechanism and Machine Theory*, **37**(11):1395-1411. [doi:10.1016/S0094-114X(02)00044-7]

Gosselin, C., 1990. Determination of the workspace of 6-DOF parallel manipulators. *Journal of Mechanisms, Transmissions, and Automation in Design*, **112**(3):331-336.

Huang, Z., Li, Q.C., 2003. Structure synthesis theories of the lower-mobility parallel robot mechanism. *Journal of Chinese Science (E Edition)*, **33**(9):813-819 (in Chinese).

Huang, Z., Kong, L.F., Fang, Y.H., 1997. Theory and Control of Parallel Robot Mechanism. China Mechanical Industry Publishing Company, Beijing, p.19, 207-225 (in Chinese).

Joshi, S., Tsai, L.W., 2003. A comparison study of two 3-DOF parallel manipulators: One with three and the other with four supporting legs. *IEEE Transactions on Robotics and Automation*, **19**(2):200-209. [doi:10.1109/TRA.2003.808857]

Li, M., Huang, T., Zhang, D.W., Zhao, X.M., Hu, S.J., Chetwynd, D.G., 2005. Conceptual design and dimensional synthesis of a reconfigurable hybrid robot. *Journal of Manufacturing Science and Engineering*, **127**(3):647-653. [doi:10.1115/1.1947208]

Liu, X.J., Wang, J.S., Pritschow, G., 2005. A new family of spatical 3-DOF fully-parallel manipulators with high rotational capability. *Mechanism and Machine Theory*, **40**(4):475-494. [doi:10.1016/j.mechmachtheory.2004.10.001]

Peng, B.B., Gao, F., 2006. Input/output velocity and force of five axes parallel machine tool. *Chinese Journal of Mechanical Engineering*, **42**(9):160-163 (in Chinese).

Shen, H.P., Yang, T.L., Tao, S.L., Liu, A.X., Ma, L.Z., 2005. Structure and displacement analysis of a novel three-translation parallel mechanism. *Mechanism and Machine Theory*, **40**:1181-1194.

Tsai, K.J., Lin, J.C., 2006. Determining the compatible orientation workspace of Stewart-Gough parallel manipulators. *Mechanism and Machine Theory*, **41**(10):1168-1184. [doi:10.1016/j.mechmachtheory.2005.12.002]

Wang, Z., Wang, Z.X., Liu, W.T., Lei, Y.C., 2001. A study on workspace, boundary workspace analysis and workpiece positioning for parallel machine tools. *Mechanism and Machine Theory*, **36**(5):605-622. [doi:10.1016/S0094-114X(01)00009-X]

Zhang, D., Gosselin, C.M., 2002. Kinetostatic analysis and design optimization of the tricept machine tool family. *Journal of Manufacturing Science and Engineering*, **124**(3):725-733. [doi:10.1115/1.1471529]